Interaction of Separated Plumes from a Horizontal Fin with Downstream Thermal Boundary Layer in a Differentially Heated Cavity

Yang Liu, Chengwang Lei and John C. Patterson

School of Civil Engineering

The University of Sydney, Sydney, NSW 2006, Australia

Abstract

A horizontal adiabatic thin fin has been adopted previously in a differentially heated cavity to enhance heat transfer through the sidewalls of the cavity. The interaction of plumes separating from the horizontal thin fin with the downstream thermal boundary layer is numerically investigated in this study. The quasi-steady state flow is concerned. Based on the numerical results, the temporal and spatial evolution of the separating plumes above the fin and the process by which they merge into the downstream boundary layer are described. It is demonstrated that the plumes induce strong oscillations in the downstream boundary layer. For the particular case considered here, the plume separation frequency is found to be 0.073-Hz. The signal of this frequency is amplified along the boundary layer flow, whereas its harmonic signal of 0.146-Hz is decayed. Through a direct stability analysis, it is revealed that the downstream boundary layer can only support signals over a narrow band of frequencies, within which the primary separation frequency of 0.073-Hz lies but its harmonic component does not.

Introduction

Natural convection flow in a differentially heated cavity is a classical heat transfer problem because of its underlying fundamental fluid mechanics and wide industrial applications, such as in solar collectors and nuclear reactors. This problem has been studied for several decades since it was first investigated in the 1950s [1].

It is demonstrated that heat transfer through the differentially heated cavity can be greatly enhanced by attaching a horizontal thin fin of an appropriately selected length to the sidewall. It is believed that separated plumes resulting from a Rayleigh-Benard type instability in the unstable thermal flow above the thin fin are responsible for the enhancement of heat transfer in the downstream boundary layer. Even though this flow has been intensively studied experimentally [2, 3] and numerically [4], the interaction between the separated plumes and the fin downstream boundary layer is still poorly understood. Many fundamental and practically important questions such as how the separated plumes merge into the downstream boundary layer and how the plume separation frequency signal evolves along the downstream boundary layer are yet to be answered. These are the topics of the present numerical investigation.

In the reminder of this paper, the problem is first put forward followed by numerical considerations and simulation results. In the discussion section, a detailed investigation, where a direct stability analysis, similar to the work of [5], is performed to study the fin downstream boundary layer characteristics.

Problem Statement

The problem under consideration is a differentially heated cavity with two thin fins horizontally placed at the heated and cooled sidewalls respectively (refer to figure 1). The cavity ceiling and bottom are adiabatic. The length of the cavity L is 1-m and the height H is 0.24-m. The thin fins attached to the sidewalls are 0.04-m long. These dimensions are adopted based on the experimental model used in [2]. The fluid is initially stationary and isothermal at temperature T_0. The temperatures of the heated and cooled sidewalls are $T_h=T_0+\triangle T/2$ and $T_c=T_0-\triangle T/2$, respectively. There are three dimensionless parameters characterising the cavity flow: the Rayleigh number (Ra), the Prandtl number (Pr) and the cavity aspect ratio (A):

$$Ra = \frac{g\beta(T_h - T_c)H^3}{\nu\kappa}, \quad Pr = \frac{\nu}{\kappa}, \quad A = \frac{H}{L}.$$

where g, β, v and k are gravitational acceleration, thermal expansion coefficient, kinematic viscosity and thermal diffusivity, respectively. The cavity is filled with water and the Prandtl number is fixed at 6.64. The Rayleigh number calculated here is 1.84×10^9.
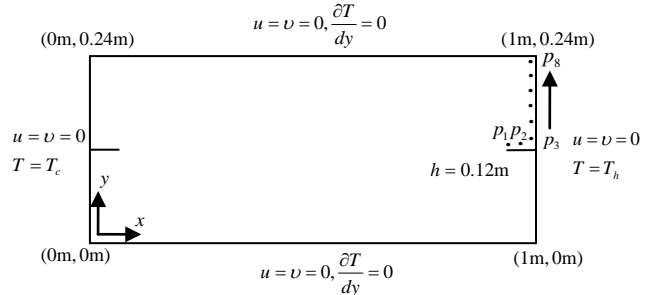
Figure 1 Schematic of the computational domain and monitoring positions: p1 (0.98m, 0.125m), p2 (0.99m, 0.125m), p3 (0.998 m, 0.13m), p4 (0.998m, 0.14m), p5 (0.998m, 0.18m), p6 (0.998m, 0.2m), p7 (0.998m, 0.22m), p8 (0.998m, 0.23m).

Numerical Considerations

It has been demonstrated that this flow configuration can be described by a two-dimensional numerical model as suggested in [4]. The governing equations are given as below, where the Boussinesq approximation is employed:

$$\frac{\partial u}{\partial x} + \frac{\partial \upsilon}{\partial y} = 0 \tag{1}$$

$$\frac{\partial u}{\partial t} + u\frac{\partial u}{\partial x} + \upsilon\frac{\partial u}{\partial y} = -\frac{1}{\rho}\frac{\partial p}{\partial x} + \nu(\frac{\partial^2 u}{\partial x^2} + \frac{\partial^2 u}{\partial y^2}) \tag{2}$$

$$\frac{\partial \upsilon}{\partial t} + u\frac{\partial \upsilon}{\partial x} + \upsilon\frac{\partial \upsilon}{\partial y} = -\frac{1}{\rho}\frac{\partial p}{\partial y} + \nu(\frac{\partial^2 \upsilon}{\partial x^2} + \frac{\partial^2 \upsilon}{\partial y^2}) + g\beta(T-T_0) \tag{3}$$

$$\frac{\partial T}{\partial t} + u\frac{\partial T}{\partial x} + \upsilon\frac{\partial T}{\partial y} = \kappa(\frac{\partial^2 T}{\partial x^2} + \frac{\partial^2 T}{\partial y^2}) \tag{4}$$

where u and υ are the velocity components in x and y directions respectively, and ρ, t, p and T are the density, time, pressure and temperature, respectively. A high temperature T_h is imposed at the right sidewall and a low temperature T_c is imposed at the left

sidewall. The ceiling and bottom are adiabatic. All surfaces are rigid and no-slip. The momentum and energy governing equations are discretized using the QUICK scheme. A second order implicit scheme is employed for the transient formulation. The SIMPLE algorithm is applied for the pressure-velocity coupling. The governing equations are solved iteratively using the ANSYS-Fluent platform and the normalised convergence criteria – the residuals are set to 10^{-6} for the energy equation and 10^{-3} for all the other equations.

A structured grid is established in the computational domain with finer mesh in the wall and fin vicinities and the time step for transient simulation is 0.05 s. The mesh and time-step adopted in this study are determined according to the numerical tests reported in [4, 6], which have shown a good agreement between the numerical and experimental data.

Numerical Simulation Results

The transient flow development downstream of the fin may be roughly classified into three stages, i.e. early stage, transitional stage and quasi-steady stage (periodic stage). The details about the first two stages have been extensively discussed in [4] and thus are not repeated here.

Following the transitional stage, periodic intermittent plume separation, resulting from an unstable thermal layer above the thin fin, has been observed experimentally with a shadowgraph method [2, 3]. Figure 2 illustrates isotherms from the current numerical simulation indicating the detailed plume separation process over one cycle. Starting from 8706-s, the plume is seen to be forming and a clear hump above the fin is observed (refer to figure 2a). With the passage of time, the plume is separated and moves towards the heated sidewall due to the entrainment effect of the downstream boundary layer. At 8713-s, the plume almost reattaches to the downstream boundary layer. At this instance, the plume compresses the downstream thermal boundary layer and the reattachment process interrupts the normal boundary layer development and separates the boundary layer into two parts. The result of the reattachment is that two parts of the boundary layer downstream of the fin are thickened. Below the reattachment point, the reattachment reduces the convection. In the meantime, heat is still continuously conducted in through the heated sidewall and hot fluid has to accumulate in this region. As a consequence, the lower part of the downstream thermal boundary layer thickens. The thermal boundary layer downstream of the attachment point loses the supply of mass flux from the lower part. Due to the heat conducted in through the sidewall, the upper part is thickened as well, as shown in figure 2d-2e. With the plume merging into the boundary layer, the reattachment effect diminishes in the mean time. The two thickening processes have different outcomes: the lower one eventually becomes a travelling wave and the upper one just turns to be a relatively small-amplitude single wave front, as seen in figure 2e.

(a) 8706s   (b) 8709s   (c) 8713s

(d) 8714s   (e) 8715s   (f) 8720s
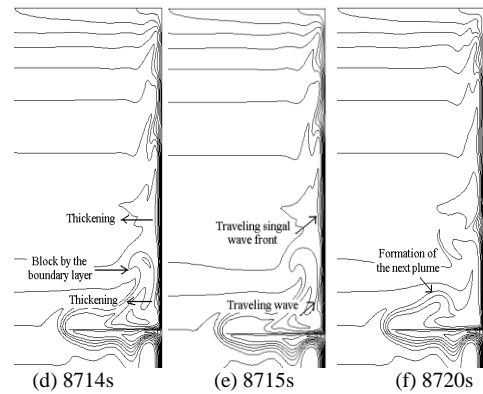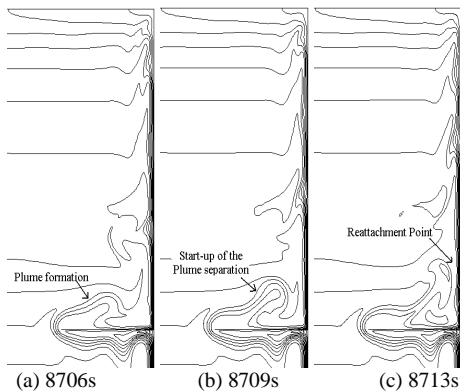
Figure 2. Plume separation development indicated by isotherms.

The temperature time series at various monitoring points indicated in figure 1 and the corresponding power spectra are presented in figure 3. It can be seen in this figure that there is one very distinct power peak at 0.073-Hz at all the monitored points. This is the plume separation frequency, which can also be estimated from the above described plume separation process. Figure 2 suggests that it takes a little less than 14-s for one plume separation cycle to complete and the corresponding frequency is then estimated to be approximately 1/14-s=0.071-Hz. From point 2 onwards, another high frequency signal appears which is twice the plume separation frequency. We can also discern two peaks from the temperature time series from point 2 to point 8. The 0.146-Hz high frequency is actually the harmonic of the separation frequency and it reflects the single wave front motion. Its power keeps growing until point 4 and then decreases as the flow approaches the ceiling. A similar phenomenon was also observed in the experiments of [3]. Also, it is noticed that the absolute power value of the f_{peak}=0.073-Hz signal increases from point 1 to point 8 (from about 8.4×10^{-3} to 3.1×10^{-2}) along the streamwise direction. However, the harmonic signal $2f_{peak}$=0.146-Hz, is first amplified and then damped. Further discussions regarding the reason for temperature signal power variations are given in the next section.
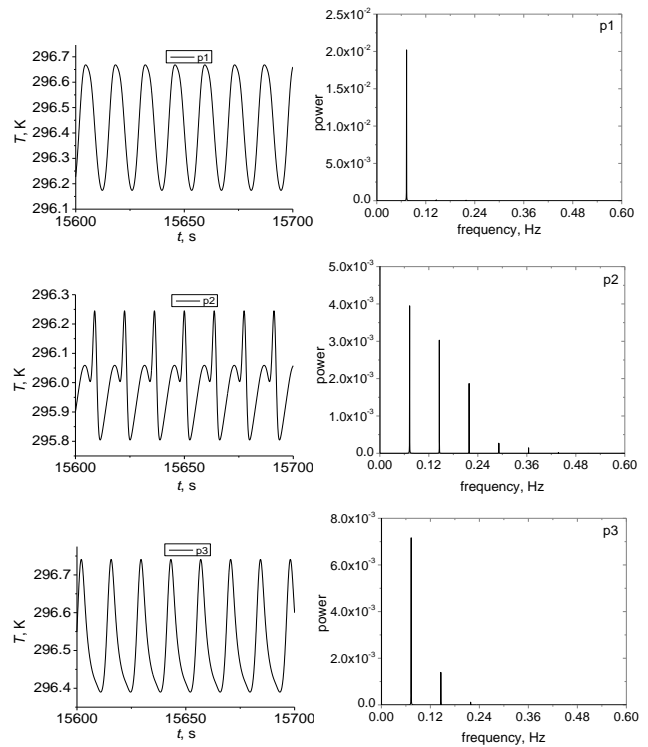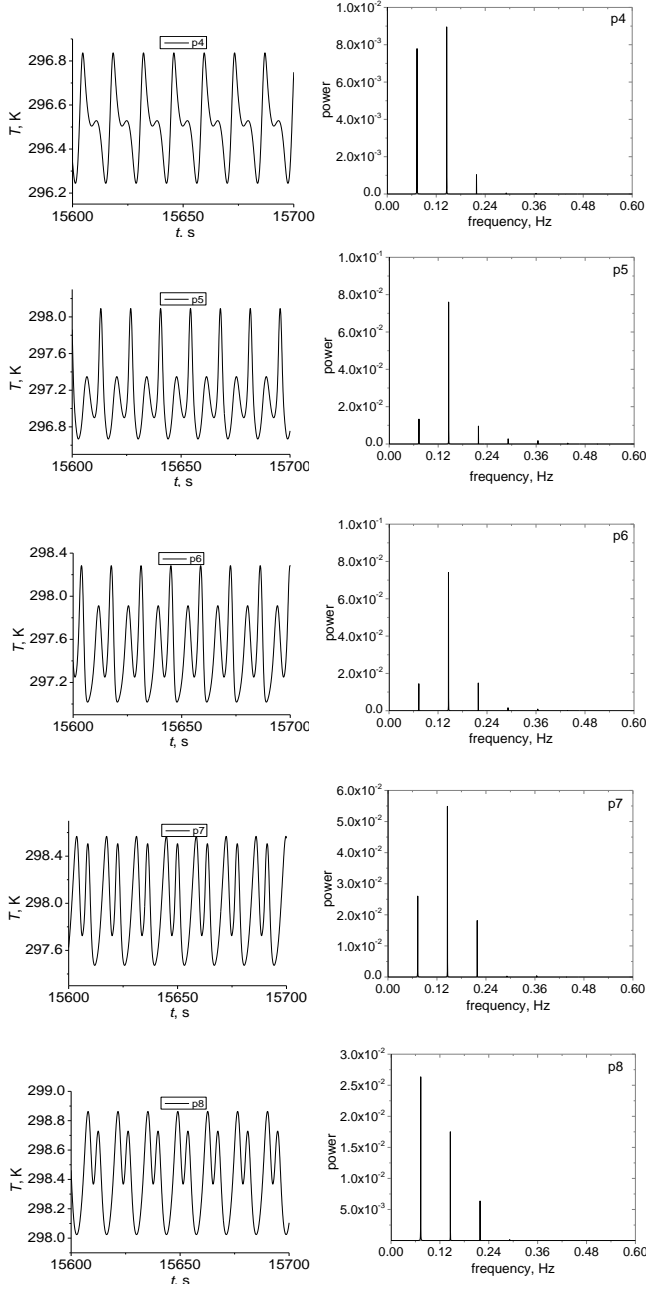
Figure 3. Temperature time series and power spectra at the monitoring points.

As stated above, the harmonic signal $2f_{peak}$ reflects the single wave front motion. However, we also find this high frequency signal at point 2 where this effect is not present. This may be due to a weak signal travelling back from point 3. The Froude number characterizing the flow regime is defined in equation 5 below, where, in the present study, D and V are the thickness and velocity magnitude of the unstable thermal layer above the fin, respectively. From the numerical simulation the unstable layer thickness is 9.22-mm and the averaged velocity magnitude across that thickness is 2.4-mm/s. Accordingly, the Froude number is estimated as 0.008 much smaller than unity, which corresponds to a sub-critical flow condition, allowing the flow disturbance to travel back upstream.

$$Fr = \frac{V}{\sqrt{gD}} \tag{5}$$

Discussions

It is revealed above that the 0.073-Hz and 0.146-Hz signals at the fin downstream correspond to the travelling waves and travelling single wave fronts respectively. The spectral analysis shows that the power of the 0.073-Hz signal keeps increasing in the flow direction and its harmonic frequency signal first increases and then decreases along the flow direction. The cause of the different spectral behaviours is discussed in this section.

As is well known, the thermal boundary layer either amplifies or damps a signal of a particular frequency. Since in the present case both the two travelling signals are convected through the downstream boundary layer, it is of great importance to understand how the downstream boundary layer responds to external signals. For this purpose, a non-finned 1-m$\times$0.12-m cavity (see figure 4), which is equivalent to the upper half of the finned cavity described above, is calculated. The temperatures of the heated and cooled sidewalls are T_h and T_0, respectively. All fluid properties and numerical procedures remain the same as those in the above 0.24-m high finned cavity calculation. This configuration will result in similar temperature stratification at the steady or quasi-steady state to the upper half of the finned cavity, and thus allow us to relate the response of the thermal boundary layer in the half cavity case to the downstream thermal boundary layer of the finned cavity.

Temperatures are monitored at three locations 2-mm away from the heated sidewall (refer to figure 4). The heights of point 1 to 3 are 0.01-m, 0.06-m and 0.1-m respectively. A direct stability analysis is performed to study the response of the thermal boundary layer adjacent to the heated sidewall after the cavity scale temperature stratification is established. Two types of perturbations, i.e. random and single mode perturbations, are considered here. The perturbations are added to the energy governing equation in a region of 1.5-mm$\times$1.5-mm at the lower corner of the heated sidewall. A similar approach has been adopted in [5] and the details are thus not repeated in this paper.
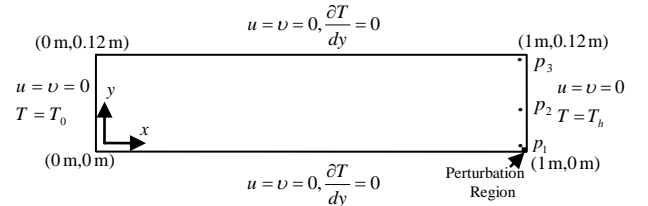
Figure 4. Schematic of the 0.12-m$\times$1-m cavity.

The characteristic frequency band of the boundary layer can be found through the random perturbation test. Figure 5 illustrates temperature time series and the corresponding power spectra of FFT at the three monitoring points.

It can be found in this figure that the temperature oscillation increases along the flow direction, as indicated by the increasing power values in the spectra. This suggests that the boundary layer is convectively unstable under the current parameter setting. Also, we can see that the boundary layer exhibits a band of frequency response approximately ranging from 0.06-Hz to 0.15-Hz to the random perturbation. To precisely determine the boundary layer response to different signals, a series of single mode perturbation tests are also performed.
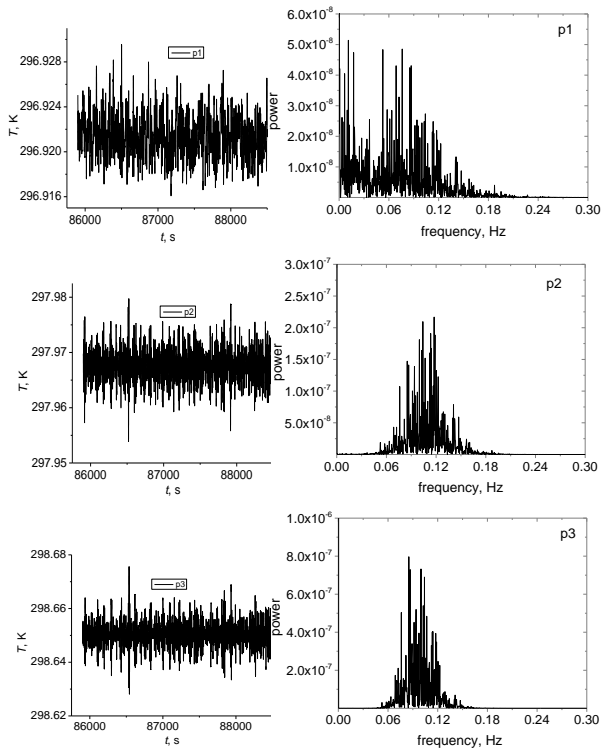
Figure 5. Temperature time series and power spectra of random mode perturbation test.

In the single mode perturbation test, sinusoidal perturbations of a range of frequencies are introduced at the same location as indicated in figure 4. Totally twelve frequencies are tested, i.e. from 0.04-Hz to 0.15-Hz with a step of 0.01-Hz, which cover the f_{peak} and $2f_{peak}$ signals. Figure 6 illustrates the temperature oscillation amplitude at point 1 and point 3 obtained with single-mode perturbations of the same intensity but different frequencies. It can be seen that only perturbations over a certain range of frequencies are amplified by the boundary layer and perturbations with frequencies outside that range decay. It can be discerned that a perturbation of 0.07-Hz is be the most amplified one while a perturbation of 0.14-Hz would be decays.
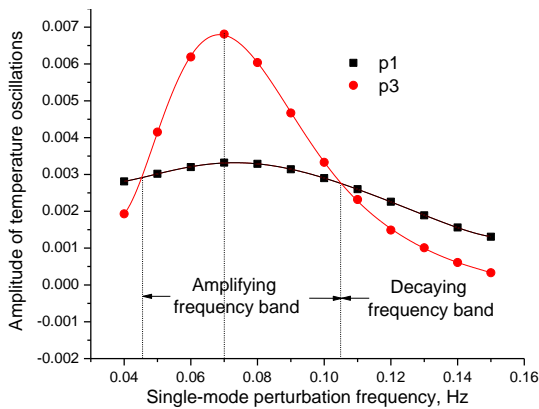
Figure 6. Temperature oscillations of single mode perturbation test.

Consider the similarity between half-cavity case and the upper half of the finned cavity, the plume separation frequency is in the amplifying range of the fin downstream boundary layer, while the $2f_{peak}$ signal is not. This explains why the 0.073-Hz signal is amplified while the 0.146-Hz signal decays towards the ceiling.

Conclusions

In this paper, the separated plumes from a horizontal thin fin in a differentially heated cavity and their interactions with the downstream boundary layer are investigated numerically. The results suggest that the thermal flow above the fin is unstable and a Rayleigh-Benard type instability in the form of separated plumes is observed. The interaction between the separated plumes and the downstream thermal boundary layer leads to travelling waves and travelling single wave fronts in the downstream boundary layer. Correspondingly, two peak frequencies can be discerned from the spectra of temperature time series. Through direct stability analysis, it is confirmed that the plume separation frequency lies within the frequency band of the downstream boundary layer, and thus is amplified, whereas the harmonic component of the plume separation frequency lies outside the frequency band, and thus is decayed.

Acknowledgments

References

[1] Batchelor, G., Heat transfer by free convection across a closed cavity between vertical boundaries at different temperatures, *Quart. Appl. Math*, **12**(3), 1954, 209-233.

[2] Xu, F., J.C. Patterson, & C. Lei, An experimental study of the unsteady thermal flow around a thin fin on a sidewall of a differentially heated cavity, *International Journal of Heat and Fluid Flow*, **29**(4), 2008, 1139-1153.

[3] Xu, F., J.C. Patterson, & C. Lei, Temperature oscillations in a differentially heated cavity with and without a fin on the sidewall, *International Communications in Heat and Mass Transfer*, **37**(4), 2010, 350-359.

[4] Xu, F., J.C. Patterson, & C. Lei, Transition to a periodic flow induced by a thin fin on the sidewall of a differentially heated cavity, *International Journal of Heat and Mass Transfer*, **52**(3-4), 2009, 620-628.

[5] Armfield, S. & R. Janssen, A direct boundary-layer stability analysis of steady-state cavity convection flow, *International Journal of Heat and Fluid Flow*, **17**(6), 1996, 539-546.

[6] Xu, F., J.C. Patterson, & C. Lei, Unsteady flow and heat transfer adjacent to the sidewall wall of a differentially heated cavity with a conducting and an adiabatic fin, *International Journal of Heat and Fluid Flow*, **32**, 2011, 680-687.